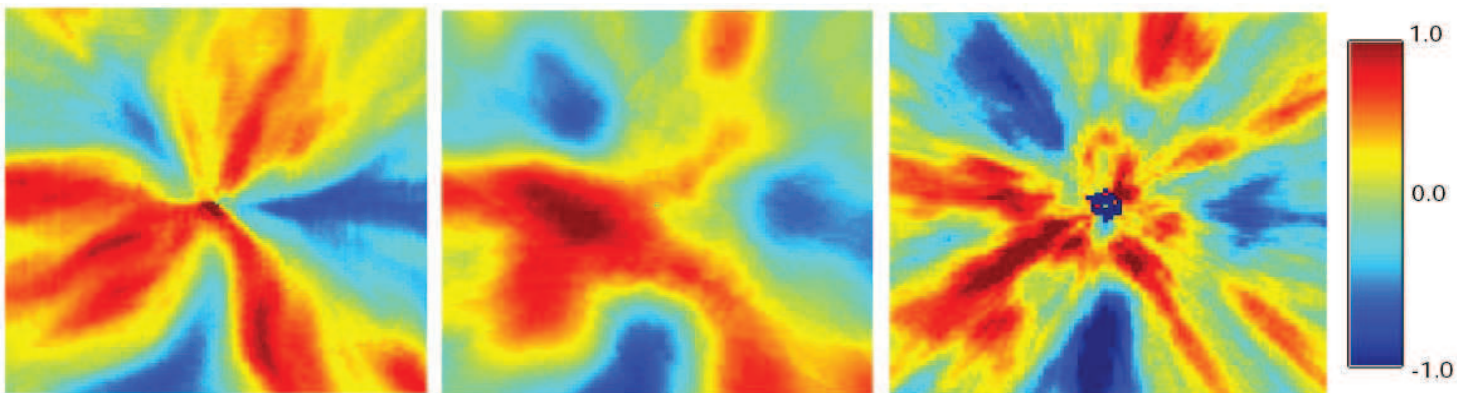


# Characterization of Spatial Heterogeneity in Groundwater Applications

**Paolo Trinchero**

**PhD Thesis**



**Supervisors:**

**Xavier Sànchez-Vila**

**Daniel Fernández-García**



**HYDROGEOLOGY GROUP**  
TECHNICAL UNIVERSITY OF CATALONIA

Characterization of spatial heterogeneity in groundwater  
applications

PhD Thesis

Department of Geotechnical Engineering and Geo-Sciences (ETCG)

Technical University of Catalonia, UPC

Paolo Trincherò

February 2009



**HYDROGEOLOGY GROUP**  
TECHNICAL UNIVERSITY OF CATALONIA

This thesis was funded by the Agència de Gestió d'Ajuts Universitaris i de Recerca of the Catalan Government (FI scholarship), Enresa and the Spanish CICYT (project PARATODO).

*Ai miei vecchi, ai miei nonni e alla Geo.*



*”Isaura, città dai mille pozzi, si presume sorga sopra un profondo lago sotterraneo. Dappertutto dove gli abitanti scavando nella terra lunghi buchi verticali sono riusciti a tirar su dell’acqua, fin là e non oltre si è estesa la città: il suo perimetro verdeggiante ripete quello delle rive buie del lago sepolto, il paesaggio invisibile condiziona quello visibile, tutto ciò che si muove al sole è spinto dall’onda che batte chiusa sotto il cielo calcareo della roccia.”*

***Italo Calvino, Le città invisibili***



# Abstract

Heterogeneity is a salient feature of every natural geological formation. In the past decades a large body of literature has focused on the effects of heterogeneity on flow and transport problems. These works have substantially improved the understanding of flow and transport phenomena but still fail to characterize many of the important features of an aquifer. Among them, preferential flows and solute paths, connectivity between two points of an aquifer, and interpretation of hydraulic and tracer tests in heterogeneous media are crucial points that need to be properly assessed to obtain accurate model predictions. In this context, the aim of this thesis is twofold:

- to improve the understanding of the effects of heterogeneity on flow and transport phenomena
- to provide new tools for characterizing aquifer heterogeneity

Also, this thesis aims to give a contribution in filling the gap between academics and practitioners. In this context, the thesis provides a series of frameworks that can be easily used by practitioners to infer qualitative and quantitative information of the underlying heterogeneous structure of the porous media.

First, we start by theoretically and numerically examine the relationship between two indicators of flow and transport connectivity. The flow connectivity indicator used here is based on the time elapsed for hydraulic response in a pumping test (e.g., the storage coefficient estimated by



the Cooper-Jacob method,  $S_{est}$ ). Regarding transport, we select the estimated porosity from the observed breakthrough curve ( $\phi_{est}$ ) in a forced-gradient tracer test. According to *Knudby and Carrera* [51] these two indicators measure connectivity differently, and are poorly correlated. Here, we use perturbation theory to analytically investigate the intrinsic relationship between  $S_{est}$  and  $\phi_{est}$ . We find that  $\phi_{est}$  can be expressed as a weighted line integral along the particle trajectory involving two parameters: the transmissivity point values,  $T$ , and the estimated values of  $S_{est}$  along the particle path. The weighting function is linear with the distance from the pumping well, thus the influence of the weighting function is maximum at the injection area, whereas the hydraulic information close to the pumping well becomes redundant (null weight). The relative importance of these two factors is explored using numerical simulations in a given synthetic aquifer and tested against intermediate-scale laboratory tracer experiments. We conclude that the degree of connectivity between two points of an aquifer (point-to-point connectivity) is a key issue for risk assessment studies aimed at predicting the travel time of a potential contaminant.

Second, a geostatistical framework has been developed to delineate connectivity patterns using a limited and sparse number of measurements. The methodology allows conditioning the results to three types of data measured over different scales, namely: (a) travel times of convergent tracer tests,  $t_a$ , (b) estimates of the storage coefficient from pumping tests interpreted using the Cooper-Jacob method,  $S_{est}$ , and (c) measurements of transmissivity point values,  $T$ . The ability of the methodology to properly delineate capture zones is assessed through estimations (i.e. ordinary cokriging) and sequential gaussian simulations based on different sets of measurements.

Third, a novel methodology for the interpretation of pumping tests in leaky aquifer systems, referred to as the double inflection point (DIP) method, is presented. The method is based on the analysis of the first and second derivatives of the drawdown with respect to log time for the estimation of the flow parameters. Like commonly used analysis procedures, such as the type-curve approach developed by *Walton* [99] and the inflection point method developed by *Hantush* [42], the mathematical development of the DIP method is based on the assumption of homogeneity of

the leaky aquifer layers. However, contrary to the two methods developed by Hantush and Walton, the new method does not need any fitting process. In homogeneous media, the two classic methods and the one proposed here provide exact results for transmissivity, storativity, and leakage factor when aquifer storage is neglected and the recharging aquifer is unperturbed. The real advantage of the DIP method comes when applying all methods independently to a test in a heterogeneous aquifer, where each method yields parameter values that are weighted differently, and thus each method provides different information about the heterogeneity distribution. Therefore, the methods are complementary and not competitive. In particular, the combination of the DIP method and Hantush method is shown to lead to the identification of contrasts between the local transmissivity in the vicinity of the well and the equivalent transmissivity of the perturbed aquifer volume.

Fourth, the meaning of the hydraulic parameters estimated from pumping test performed in leaky aquifers is assessed within a Monte Carlo framework. Pumping tests are routinely interpreted from the analysis of drawdown data and their derivatives. These interpretations result in a small number of apparent parameter values which lump the underlying heterogeneous structure of the aquifer. Key questions in such interpretations are: (1) what is the physical meaning of those lumped parameters, and (2) whether it is possible to infer some information about the spatial variability of the hydraulic parameters. The system analyzed in this paper consists of an aquifer separated from a second recharging aquifer by means of an aquitard. The natural log transforms of the transmissivity,  $\ln T$ , and the vertical conductance of the aquitard,  $\ln C$ , are modeled as two independent second-order stationary spatial random functions (SRF). The Monte Carlo approach is used to simulate the time-dependent drawdown at a suite of observation points for different values of the statistical parameters defining the SRFs. Drawdown data at each observation point are independently used to estimate hydraulic parameters using three existing methods: (i) the inflection-point method, (ii) curve fitting, and (iii) the double inflection-point method. The resulting estimated parameters are shown to be space dependent and vary with the interpretation method, since each method gives different emphasis to different parts of the time-drawdown data. Moreover, the heterogeneity in the pumped aquifer or the aquitard influences the estimates in

distinct manners. Finally, we show that by combining the parameter estimates obtained from the different analysis procedures, information about the heterogeneity of the leaky aquifer system may be inferred.

Fifth, an unsaturated highly heterogeneous waste rock pile is modeled as a simple linear system. For each lysimeter at the base of the pile for which there is a time-series of outflow, a transfer function (TF) is computed as the ratio of the output and the input (rainfall time series) normalized by a coefficient that implicitly accounts for evapotranspiration and horizontal redistribution. The empirical TF is then parametrized by separating the fast and the slow flow components. The fast component, which flows through the macropores, is assumed to be released instantaneously while the slow component (through the matrix) is simulated using a linear-reservoir model. The aim of this approach is not to describe the complexity of the medium at the local scale but to obtain a first-order identification of the averaged processes occurring within it. The calibration of the parametric model provides information on the characteristic time of the flow through the matrix and on the fraction of the water that, within each section, is channeled through the macropores. An analysis of the influence of the scale on the results is also provided showing that at large scales the behavior of the system tends to that of an equivalent matrix reservoir masking the effects of preferential flow.

# Resumen

La heterogeneidad es una característica saliente de cada formación geológica natural. En las últimas décadas un gran número de trabajos se han centrado en estudiar la influencia de la heterogeneidad en los problemas de flujo y transporte en medios poros. Dichos trabajos han mejorado sustancialmente la comprensión de los mecanismos que gobiernan estos fenómenos, sin embargo aun existen carencias en la caracterización de propiedades importantes de un acuífero. Entre ellas, el flujo preferencial, la conectividad entre dos puntos de un acuífero y la interpretación de ensayos en acuíferos heterogéneos son aspectos importantes que tienen que ser adecuadamente evaluados para obtener modelos predictivos robustos. En este contexto, el objetivo de esta tesis es doble:

- mejorar el conocimiento de la influencia de la heterogeneidad en los procesos de flujo y transporte
- proporcionar nuevas herramientas para caracterizar la heterogeneidad de los acuíferos

Asimismo, esta tesis trata de dar su pequeña contribución en acortar las distancias entre el mundo académico y las aplicaciones prácticas. Para ello proporciona una serie de marcos que pueden ser utilizadas fácilmente por los profesionales para inferir información cualitativa y cuantitativa de la heterogeneidad de un acuífero.

En primer lugar, evaluamos desde un punto de vista tanto teórico como numérico la relación entre dos indicadores de conectividad de flujo y transporte. El indicador de conectividad de flujo

utilizado aquí se basa en el tiempo de respuesta hidráulica en un ensayo de bombeo (por ejemplo, el coeficiente de almacenamiento estimado con el método de Cooper-Jacob). Como indicador de conectividad de transporte utilizamos la porosidad estimada de curvas de llegadas ( $\phi_{est}$ ) en ensayos de trazadores con flujo radial. Según *Knudby and Carrera* [51] estos dos indicadores miden la conectividad de forma diferente, y están poco correlacionados. En este capítulo se utiliza la teoría de pequeñas perturbaciones para investigar analíticamente la relación intrínseca entre  $S_{est}$  y  $\phi_{est}$ . Los resultados muestran que  $\phi_{est}$  se puede expresar como una integral de línea ponderado a lo largo de la trayectoria de las partículas. Dicha ponderación es función de dos parámetros: valores puntuales de transmisividad,  $T$ , y estimaciones de  $S$  a lo largo de la trayectoria de las partículas. La función de peso es lineal con la distancia desde el bombeo y, por lo tanto, su influencia es máxima en el área de inyección, mientras que la información hidráulica cerca de la zona de bombeo resulta ser redundante (peso nulo). La importancia relativa de estos dos parámetros se evalúa por medio de simulaciones numéricas y se contrasta con pruebas de trazadores de escala intermedia realizadas en laboratorio. Los resultados obtenidos evidencian como el grado de conectividad entre dos puntos de un acuífero (conectividad punto a punto) es un factor clave en estudios de análisis de riesgo cuyo objetivo es predecir el tiempo de viaje de un contaminante potencial.

En segundo lugar, se ha desarrollado un marco geoestadístico para delinear mapas de conectividad utilizando un número limitado de medidas hidráulicas. La metodología permite condicionar los resultados a tres tipos de datos medidos a diferentes escalas: (a) tiempos de llegada de ensayos de trazadores en flujo convergente  $t_d$ , (b) estimaciones del coeficiente de almacenamiento obtenidas de ensayos de bombeo interpretados con el método de Cooper-Jacob,  $S_{est}$ , y (c) mediciones de valores de transmisividad puntuales,  $T$ . La capacidad de la metodología para delinear correctamente zonas de captura se evalúa a través de estimaciones (krigeado simple y ordinario) y simulaciones secuenciales gaussianas basadas en diferentes conjuntos de medidas.

En tercer lugar, se ha desarrollado una nueva metodología, llamada método del doble punto de inflexión (DIP), para la interpretación de pruebas de bombeo en acuíferos semiconfinados. El

método se basa en el análisis de la primera y segunda derivada de la curva de descenso en función de logaritmo del tiempo. Al igual que los procedimientos de análisis comúnmente utilizados (método de superposición de curvas patrones de *Walton* [99] y método del punto de inflexión de *Hantush* [42]) el desarrollo matemático del método DIP se basa en la hipótesis de homogeneidad del medio. Sin embargo, contrariamente a los dos métodos desarrollados por Hantush y Walton, el nuevo método no necesita ningún proceso de ajuste. En medios homogéneos, los tres métodos proporcionan estimaciones exactas de la transmisividad, el coeficiente de almacenamiento, y el factor de goteo cuando el almacenamiento y los descensos en el acuitardo son despreciables. La verdadera ventaja de este método (DIP) se observa en acuíferos heterogéneos, cuando se aplica de forma independiente junto a las demás metodologías. En estos casos cada método proporciona estimaciones de los parámetros que están ponderados de forma diferente, y por lo tanto cada método proporciona una información diferente acerca de la heterogeneidad. Esto significa que los métodos son complementarios y no competitivos. En particular, la combinación del método DIP y el método de Hantush permite identificar contrastes entre la transmisividad local (cerca del pozo) y la transmisividad equivalente del acuífero.

En cuarto lugar, se utiliza el método de Monte Carlo para evaluar el significado de aquellos parámetros hidráulicos estimados de ensayos de bombeo en acuíferos semiconfinados. Estos ensayos suelen interpretarse utilizando datos de descenso en función del tiempo y sus derivadas. El resultado es un número limitado de parámetros aparentes que agrupan la información sobre la heterogeneidad en un único valor. Cuestiones clave en esas interpretaciones son las siguientes: (1) ¿Cuál es el significado físico de esos parámetros aparentes?, y (2) ¿es posible inferir alguna información acerca de la variabilidad espacial de los parámetros hidráulicos?. El sistema analizado en esta sección consiste en un acuífero separado de un segundo acuífero por un acuitardo. El logaritmo de la transmisividad,  $\ln T$ , y de la conductancia vertical del acuitardo,  $\ln C$ , se modelan como dos variables independientes aleatorias estacionarias de segundo orden (SRF). El enfoque de Monte Carlo se utiliza para simular los descensos transitorios en un conjunto de puntos de observación para diferentes valores de los parámetros estadísticos que definen las variables aleatorias. Los des-

censos en cada punto de observación se utilizan de forma independiente para la estimación de los parámetros hidráulicos utilizando tres métodos existentes: (i) el método del punto de inflexión, (ii) el ajuste de curvas patrones, y (iii) el método del doble punto de inflexión. Los parámetros estimados resultan ser espacialmente dependientes y varían en función del método de interpretación, ya que cada método pondera de forma distinta diferentes partes de la curva de descensos en función del tiempo. Por otra parte, la heterogeneidad del acuífero bombeado o del acuitardo influye en las estimaciones de forma distinta. Por último, se muestra que al combinar las estimaciones de los parámetros obtenidos a partir de los diferentes procedimientos de análisis, se puede inferir información sobre la heterogeneidad del sistema.

En quinto lugar, se modela el flujo no saturado en un dique de estériles utilizando un sistema lineal simple. Para cada uno de los lisímetros en la base del botadero se obtiene una función de transferencia (TF) calculada como el cociente entre el flujo de salida y de entrada (series temporales) normalizado por un coeficiente que implícitamente representa la evapotranspiración y la redistribución horizontal. La función de transferencia empírica se parametriza separando la componente de flujo rápida de la lenta. La componente rápida, que fluye a través de los macroporos, se asume ser instantánea mientras que la componente lenta (a través de la matriz) se simula mediante un modelo lineal. El objetivo de este enfoque no es describir la complejidad del medio a escala local, sino obtener una estimación de primer orden de los procesos que tienen lugar dentro del sistema. La calibración del modelo paramétrico proporciona información sobre el tiempo característico del flujo a través de la matriz y de la fracción de agua que, dentro de cada sección, se canaliza a través de los macroporos. Por último se presenta un análisis de la influencia de la escala en los resultados evidenciando como a gran escala el comportamiento del sistema tiende al de un sistema-matriz homogéneo equivalente, enmascarando los efectos del flujo preferencial.

# Agradecimientos

Prima di tutto vorrei ringraziare tutte quelle persone che durante questi quattro anni mi sono state spiritualmente vicine. Senza di loro non avrei mai finito questa tesi!!

Grazie ai miei vecchi che mi hanno sempre e comunque appoggiato in tutte le mie decisioni. Grazie alla Geo per sopportarmi nei miei (frequenti) momenti di stress. Grazie ai miei nonni, Elide, Elda e Pinin che sono ancora qua con me e Gigi che mi protegge da lassù. Grazie a Mariana e Hartmut, non solo per l'aiuto logistico (e che aiuto!!) ma soprattutto per il loro magnifico calore umano.

Voglio anche ringraziare Xavi che è sempre stato disponibile in ogni momento. E' stato un piacere lavorare con Dani (gracias Dani), con Nadim (thanks Nadim) e con Roger (thanks Roger).

Grazie infine agli amici di Barcellona, a quelli che 'los viernes divertidos' (Luit, Vane, Leo, Manu, Ale, Chifon,...) e a quelli che hanno messo la colonna sonora (Marco). Grazie anche a quelli che ho dimenticato...Spero non ve la prendiate a male!





# Table of Contents

<b>1</b>	<b>Introduction</b>	<b>1</b>
1.0.1	Thesis outline . . . . .	4
<b>2</b>	<b>Point-to-point connectivity: what we can infer from pumping and tracer tests</b>	<b>7</b>
2.1	Introduction . . . . .	7
2.2	Field and Laboratory Evidences . . . . .	12
2.2.1	Pumping tests . . . . .	12
2.2.2	Laboratory Tracer Tests . . . . .	14
2.3	Analytical Relationship Between $\phi_{est}$ and $S_{est}$ . . . . .	17
2.4	Computational Investigations . . . . .	24
2.4.1	Exploring the Applicability of the Analytical Solution . . . . .	24
2.4.2	Comparison with Laboratory Tracer Experiments . . . . .	30
2.5	An Application: Delineation of capture zones . . . . .	31
2.6	Summary and conclusions . . . . .	34
<b>3</b>	<b>A framework for the stochastic Delineation of Connectivity Patterns</b>	<b>37</b>
3.1	Introduction . . . . .	37
3.2	Problem Description . . . . .	38
3.3	Background . . . . .	39
3.4	Mathematical Development . . . . .	41
3.4.1	Conditional Estimation: Kriging . . . . .	41
3.4.2	Conditional Stochastic Simulation . . . . .	48
3.5	Numerical assessment of the method . . . . .	49
3.5.1	Numerical approach . . . . .	49

3.5.2	Results and discussion . . . . .	50
3.6	Summary and Conclusions . . . . .	55
<b>4</b>	<b>A new method for the interpretation of pumping tests in leaky aquifers</b>	<b>59</b>
4.1	Introduction . . . . .	59
4.1.1	Motivation . . . . .	59
4.1.2	Leaky aquifer hydraulics . . . . .	60
4.2	Pump tests in heterogeneous media . . . . .	61
4.3	Brief review of existing methodologies . . . . .	62
4.4	The Double Inflection Point Method . . . . .	68
4.4.1	Assumptions and Methodology . . . . .	68
4.5	Application of the DIP method to the synthetic pumping test . . . . .	71
4.6	DIP Method: A Graphical Approach . . . . .	72
4.7	Comparison of the parameter values estimated with the different methods . . . . .	75
4.8	The Double Inflection Point Method as Indicator of Low/High Permeability at the Well . . . . .	78
4.9	Summary . . . . .	83
4.10	Appendix - Symmetry of the Second Derivative of the Drawdown Curve . . . . .	84
4.11	Appendix - Sensitivity Analysis of the DIP Method . . . . .	85
<b>5</b>	<b>Influence of Heterogeneity on the Interpretation of Pumping Test Data in Leaky Aquifers</b>	<b>87</b>
5.1	Introduction . . . . .	87
5.2	Problem Statement . . . . .	88
5.2.1	Existing Parameter Interpretation Methods . . . . .	88
5.2.2	Numerical Setup . . . . .	90
5.3	Results . . . . .	91
5.3.1	Impact of Aquifer Heterogeneity . . . . .	91
5.3.2	Spatial Variability of the Estimated Flow Parameters . . . . .	96
5.3.3	Identification of the Local Transmissivity at the Pumping Well . . . . .	102
5.3.4	Impact of Aquitard Heterogeneity . . . . .	104
5.4	Conclusions . . . . .	108

---

<b>6 Assessing preferential flow through an unsaturated waste rock pile using spectral analysis</b>	<b>113</b>
6.1 Introduction . . . . .	113
6.2 Study area and monitoring scheme . . . . .	115
6.3 Modeling approach . . . . .	117
6.3.1 General overview of the methodology . . . . .	117
6.3.2 Estimation of the $TF$ . . . . .	118
6.3.3 Data analysis . . . . .	119
6.3.4 Conceptual model . . . . .	120
6.4 Results and discussion . . . . .	123
6.5 Conclusions . . . . .	129
<b>7 Conclusions</b>	<b>133</b>
<b>Bibliography</b>	<b>147</b>



# List of Figures

2.1	Drawdown curves of a pumping test performed in a fractured media in Spain. In the small box it is represented the space location of the well, W, and the three piezometers, P1, P2 and P3. In a homogeneous medium the three curves would collapse. . . . .	13
2.2	Shape of the weighting function $U(r_o, \theta_o, \rho, \varphi)$ (Equation 2.4) (a) and profile along the indicated sections (b) for a well located in the origin (0, 0) and a observation point in (1, 0). $U(r_o, \theta_o, \rho, \varphi)$ is positive inside the circle defined by the pumping and observation well, and negative outside (being 0 along the circle itself). The points corresponding to the two wells are singular. . . . .	15
2.3	Transmissivity field of the sand box and location of the ports. Four sand types were used, dark indicating higher transmissivity values ( $62m^2/day$ , $22m^2/day$ , $7m^2/day$ and $2m^2/day$ respectively). The position of the well (W) and the observation points or ports (P) are indicated. . . . .	17
2.4	Normalized breakthrough curves obtained at different injection location: $t_D$ is the dimensionless time ( $t_D = Qt/\pi r^2 b \phi$ ), where $Q$ is the pumping rate, $r$ the distance from the well, $b$ the aquifer thickness and $\phi$ the actual porosity. In a homogeneous media all curves should superimpose. . . . .	18
2.5	Natural logarithm of the transmissivity field (a) and map of $S_{est}/S$ for the given aquifer (b), modified from <i>Sanchez-Vila et al.</i> [83]. Each map is representative of a subdomain of $101 \times 101$ cells centred around the well. . . . .	25
2.6	Estimated porosity, $\phi_{est}$ in each cell of a subdomain of $101 \times 101$ cells centred around the well. The porosity is computed (a) numerically using a purely advective model and (2.5), (b) numerically using an advection-dispersion model and (2.5). The values are compared with $\phi_{est}^I$ (c) from Equation (2.27) and $\phi_{est}$ (d) from Equation (2.26). All values are normalized by $\phi$ . . . . .	26

2.7	(a) Transmissivity field, (b) porosity estimated numerically using Equation (2.5), porosity estimated $\phi_{est}^{II}$ using Equation (2.28) with (c) $\alpha = 1/4$ , (d) $\alpha = 1/2$ , (e) $\alpha = 2/3$ and (f) $\alpha = 1$ . Each map is representative of a subdomain of $101 \times 101$ cells centred around the well. . . . .	28
2.8	Natural logarithm of the estimated porosity from laboratory, $\ln \phi_{est}$ , versus the natural logarithm of the transmissivity estimated using Equation (2.27) ( $\ln \phi_{est}^I$ ). The linear trendline and the correlation coefficient ( $r^2$ ) are indicated. . . . .	31
2.9	Identification of the 50 days travel time capture zone from a well located at (50, 50). The numerical results have been obtained with backward simulations using (a) a purely advective model and (b) an advection-dispersion model. The analytical complete and simplified solutions refer to Equation (2.26) and (2.27) respectively. . . . .	33
3.1	(a) Real connectivity patterns ( $\tau'$ ) and connectivity patterns estimated/simulated using (b) ordinary cokriging and (c) sequential gaussian simulation (realization 200) for scenario C. . . . .	51
3.2	Capture zone probability maps. The isoprobability contours are computed using the 300 gaussian sequential simulations for (a) scenario A, (b) scenario B and (c) scenario C. The capture zone estimated using ordinary cokriging (blue line), the real shape of the capture zone (red line) and the capture zone associated to the equivalent homogeneous field ( $T = T_G = 1m^2/day$ ) (green line) are also shown. . . . .	52
3.3	Capture zone probability maps for scenario A (gray lines) and scenario B (red lines). The real shape of the capture zone (green line) is also shown. . . . .	53
3.4	Conditional cumulative density function, ccdf, of (a) $e_{miss}$ (Equation 3.42) and (b) $e_{over}$ (Equation 3.43) for the set of 300 conditional simulations of the three scenarios. . . . .	54
4.1	logarithm base-10 of the inner part of the transmissivity field (200 by 200 grid cells out of 481 X 481) and zoom around the well location. The well, W, and observation point, P, are indicated. . . . .	63
4.2	Interpretation of the synthetic pumping test using the type curve method of <i>Walton</i> [99] . The fit curve is that for (a) $r/B = 1.5$ and (b) $r/B = 2.0$ which shows the subjectivity of the curve matching method. . . . .	64
4.3	Plot of the ratio $s_{steady}/m$ as a function of $r/B$ (equation 4.2) used in the interpretation data with the inflection point method [42]. . . . .	67
4.4	Drawdown in the synthetic pumping test and its first derivative. . . . .	67
4.5	Interpretation of the synthetic example using the DIP method. . . . .	71

4.6	DIP graphical approach: type curves of $t_{D0}$ , $t_{D1}$ and $t_{D2}$ as a function of $r/B$ . The points are the $t_{inf}$ , $t_{s1}$ and $t_{s2}$ values of the synthetic example. Note that because of the heterogeneity in the transmissivity field, it is not possible for the three points to simultaneously match the theoretical curves. . . . .	74
4.7	Percent error in the estimation of the leakage factor as a function of $r/B$ for two different relative errors in the estimation of $\tau_j$ . . . . .	75
4.8	Second derivative of the drawdown from the synthetic pumping test in the heterogeneous aquifer and in the equivalent homogeneous aquifer (defined in terms of the geometric mean of the transmissivity field). The error bars show the shift of the singular points $t_{inf}$ , $t_{s1}$ and $t_{s2}$ . . . . .	76
4.9	$r/B$ as a function of the $\tau_j$ values. . . . .	77
4.10	Estimates of the (a) leakage factor and (b) transmissivity using the different methodologies. $B_W$ and $T_W$ are the leakage factor and the transmissivity at the well, respectively. . . . .	78
4.11	Leakage factor (normalized on the regional geometric mean of transmissivity) as a function of the well distance estimated using the DIP ( $t_{s1}$ and $t_{s2}$ ) and Hantush inflection point methods. The ratio between the transmissivity at the well and the mean transmissivity value is 2. . . . .	80
4.12	Leakage factor (normalized on the regional geometric mean of transmissivity) as a function of the well distance estimated using the DIP ( $t_{s1}$ and $t_{s2}$ ) and Hantush inflection point methods. The ratio between the transmissivity at the well and the mean transmissivity value is 0.5. . . . .	81
5.1	Normalized transmissivity estimates using the inflection-point and the curve fitting methods for different distances from the pumping well (heterogeneous aquifer with geometric mean, $T_g = 1m^2/day$ , $\ln T$ integral scale $I = 8m$ , $\sigma^2 = 1$ , and a uniform aquitard with $Co = 0.001day^{-1}$ ). . . . .	92
5.2	Normalized aquitard conductance estimated using the inflection-point and the curve fitting methods for different distances from the pumping well (heterogeneous aquifer with $T_g = 1m^2day^{-1}$ , $I = 8m$ , and $\sigma^2 = 1$ , and a uniform aquitard with $Co = 0.001day^{-1}$ ). . . . .	93
5.3	Probability density function of $T/T_g$ estimated using the inflection-point method at different distances from the well. The lognormal $LN(0, 1)$ distribution is also shown. (heterogeneous aquifer with $T_g = 1m^2day^{-1}$ , $I = 8m$ , and $\sigma^2 = 1$ , and a uniform aquitard with $Co = 0.001day^{-1}$ ). . . . .	95



5.4	Sensitivity of the $T/T_g$ pdf estimated using the inflection-point method to the conductance and log-transmissivity integral scale and variance. The lognormal distribution $LN(0, 1)$ is also shown. . . . .	96
5.5	(a) Leakage factor normalized by $B_g = (T_g/C_o)^{1/2}$ and (b) transmissivity normalized by $T_g$ estimated using the inflection-point method for randomly selected simulations as a function of distance from the well. . . . .	97
5.6	Expected value of the (a) Leakage factor normalized by $B_g = (T_g/C_o)^{1/2}$ and (b) transmissivity normalized by $T_g$ as a function of distance from the well (heterogeneous aquifer with $T_g = 1m2day^{-1}$ , $I = 8m$ , and $\sigma^2 = 1$ , and a uniform aquitard with $C_o = 0.001day^{-1}$ ). . . . .	99
5.7	Comparison of the mean steady state drawdown and drawdown slope at the inflection-point for a case of spatially variable transmissivity to that of the homogeneous aquifer with transmissivity $T_g$ . . . . .	101
5.8	Normalized transmissivity estimated using the inflection-point and the DIP1 (positive peak) methods for $r/I = 1/2$ and $r/I = 2$ (heterogeneous aquifer with $T_g = 1m2day^{-1}$ , $I = 8m$ , and $\sigma^2 = 1$ , and a uniform aquitard with $C_o = 0.001day^{-1}$ ).102	
5.9	Normalized transmissivity estimated using the inflection-point and the DIP2 (negative peak) method for $r/I=1/2$ and $r/I=2$ (heterogeneous aquifer with $T_g = 1m2day^{-1}$ , $I = 8m$ , and $\sigma^2 = 1$ , and a uniform aquitard with $C_o = 0.001day^{-1}$ ). . . . .	103
5.10	Normalized transmissivity estimated using the inflection-point method and the geometric mean of the two DIP estimates for $r/I = 1/2$ and $r/I = 2$ (heterogeneous aquifer with $T_g = 1m2day^{-1}$ , $I = 8m$ , and $\sigma^2 = 1$ , and a uniform aquitard with $C_o = 0.001day^{-1}$ ). . . . .	103
5.11	Correlation of the difference in the estimated transmissivity values obtained from different methods to the transmissivity at the well (heterogeneous aquifer with $T_g = 1m2day^{-1}$ , $I = 8m$ , and $\sigma^2 = 1$ , and a uniform aquitard with $C_o = 0.001day^{-1}$ ).105	
5.12	Normalized transmissivity estimated using the inflection-point and the curve fitting methods for different distances from the pumping well (uniform aquifer with $T_o = 1m^2/day$ , and spatially variable aquitard with $C_g = 0.01day^{-1}$ , $I = 8m$ , and $\sigma^2 = 1$ ) . . . . .	107
5.13	Normalized aquitard conductance estimated using the inflection-point and the curve fitting methods for different distances from the pumping well (uniform aquifer with $T_o = 1m^2/day$ , and spatially variable aquitard with $C_g = 0.01day^{-1}$ , $I = 8m$ , and $\sigma^2 = 1$ ). . . . .	108

---

5.14	Leaky well function and vertical flow through the aquitard as a fraction of the pumping rate vs. $r/B$ at the inflection point $t_p = r_{obs}S B/2T$ for different values of $r_{obs}/B$ . . . . .	109
6.1	Simplified cross section of constructed pile experiment and plan view of experiment core (inset A). . . . .	116
6.2	Periodogram of the rainfall (a) and of the outflow through lysimeter 9 (b). . . . .	119
6.3	Dimensionless parametric TF as a function of different $\alpha$ values. . . . .	123
6.4	Periodogram of the outflow through lysimeter 8 and 9 (a) and outflow through the same lysimeter after the application of a single artificial rainfall event (indicated by the arrow) (b) . . . . .	124
6.5	Empirical TF (dotted line) and simulated TF (solid line) for each lysimeter . . . . .	125
6.6	Water released during the period considered (March 1 - October 30, 2000) versus calibrated $\alpha$ . . . . .	128
6.7	Location of the lysimeters aggregated into quarters . . . . .	128
6.8	Empirical TF (dotted line) and simulated TF (solid line) for the quarters (a) SW, (b) NW, (c) SE and (d) NE. . . . .	129
6.9	Empirical TF (dotted line) and simulated TF (solid line) of the all lysimeters aggregated into one. . . . .	130



# List of Tables

2.1	Interpretation of the pumping test of figure 2.1 using the Cooper-Jacob method. . . . .	14
4.1	summary of the results obtained with each method. DIP1 and DIP2 are the results obtained using the DIP method with $t_{s1}$ and $t_{s2}$ respectively. DIP mean refers to the geometric mean of DIP1 and DIP2. The geometric mean is the spatial mean of the parameter used in the generation of time-drawdown data. . . . .	72
5.1	Expected value and standard deviation (shown in parenthesis) of the flow parameters function of distance from the well- Case of spatially variable aquifer. . . . .	94
5.2	Expected value and standard deviation (shown in parenthesis) of the flow parameters function of distance from the well- Case of spatially variable aquitard. . . . .	106
6.1	Summary of the water released by each lysimeter during the period considered and ratio $\mu$ of the water released divided by the volume of precipitation corresponding to each section ( $1.29 m^3$ ) . . . . .	120
6.2	results of the calibration for each individual lysimeter . . . . .	124
6.3	results of the calibration for a combination of four lysimeters aggregated (see Figure 6.7) . . . . .	127

